BIOCHEMISTRY
including biophysical chemistry & molecular biology
Article

Biochemistry **2010,** *49,* 49–57 49
DOI: 10.1021/bi9017285

Paramagnetic ^{13}C and ^{15}N NMR Analyses of the Push and Pull Effects in Cytochrome *c* Peroxidase and *Coprinus cinereus* Peroxidase Variants: Functional Roles of Highly Conserved Amino Acids around Heme[†]

Daisuke Nonaka,[‡] Hiroyuki Wariishi,[§] Karen G. Welinder,[∥] and Hiroshi Fujii*,[‡]

[‡]*Institute for Molecular Science and Okazaki Institute for Integrative Bioscience, National Institutes of Natural Sciences, Myodaiji, Okazaki 444-8787, Japan,* [§]*Faculty of Agriculture, Kyushu University, Hakozaki, Fukuoka 821-8581, Japan, and* [∥]*Department of Biotechnology, Chemistry and Environmental Engineering, Aalborg University, Sohngaardsholmsvej 49, DK-9000 Aalborg, Denmark*

Received October 7, 2009; Revised Manuscript Received November 30, 2009

ABSTRACT: Paramagnetic ^{13}C and ^{15}N nuclear magnetic resonance (NMR) spectroscopy of heme-bound cyanide ($^{13}C^{15}N$) was applied to 11 cytochrome *c* peroxidase (CcP) and *Coprinus cinereus* peroxidase (CIP) mutants to investigate contributions to the push and pull effects of conserved amino acids around heme. The ^{13}C and ^{15}N NMR data for the distal His and Arg mutants indicated that distal His is the key amino acid residue creating the strong pull effect and that distal Arg assists. The mutation of distal Trp of CcP to Phe, the amino acid at this position in CIP, changed the push and pull effects so they resembled those of CIP, whereas the mutation of distal Phe of CIP to Trp changed this mutant to become CcP-like. The ^{13}C NMR shifts for the proximal Asp mutants clearly showed that the proximal Asp−His hydrogen bonding strengthens the push effect. However, even in the absence of a hydrogen bond, the push effect of proximal His in peroxidase is significantly stronger than in globins. Comparison of these NMR data with the compound I formation rate constants and crystal structures of these mutants showed that (1) the base catalysis of the distal His is more critical for rapid compound I formation than its acid catalysis, (2) the primary function of the distal Arg is to maintain the distal heme pocket in favor of rapid compound I formation via hydrogen bonding, and (3) the push effect is the major contributor to the differential rates of compound I formation in wild-type peroxidases.

Heme peroxidases are ubiquitous enzymes that catalyze one-electron oxidation of various organic and inorganic compounds at the expense of hydrogen peroxide (*1*−*4*). The most characteristic feature of peroxidases is fast reaction with hydrogen peroxide in a 1:1 manner to form a reactive intermediate, compound I. The reaction between peroxidase and hydrogen peroxide is best visualized as occurring in two steps (*5*):

$$\mathrm{Prx(Fe^{3+})\ (resting\ state) + H_2O_2 \rightarrow Prx(Fe^{3+})-OOH}$$
$$\rightarrow \mathrm{Prx(Fe^{4+}{=}O), R\bullet (compound\ I) + H_2O}$$

In the first step, hydrogen peroxide binds to heme iron of the resting state enzyme forming a ferric hydroperoxide intermediate. Two of the water molecules in the distal heme pocket are replaced by an incoming hydrogen peroxide, and then His at the distal side of heme (the distal His) accepts a proton from the incoming hydrogen peroxide to assist the binding of the peroxide anion to ferric heme iron. During hydrogen peroxide diffusion and water replacement, considerable energy is spent on reorganization of the distal heme pocket. In the second step, the O−O bond of the ferric hydroperoxide intermediate is cleaved, producing compound I and water (Figure 1) (*6*). The O−O bond cleavage step is facilitated by preorganized hydrogen bonding interactions from the distal His and Arg, called the pull effect, and donation of an electron from the proximal His, called the push effect (*5*). As a result, the O−O bond cleavage step is very fast for wild-type peroxidases, probably on the order of $10^5\ s^{-1}$ at room temperature (*7*). Under typical stopped-flow conditions, keeping the observed pseudo-first-order rate constant of compound I formation less than $300\ s^{-1}$, the association of hydrogen peroxide (the first step) is the rate-limiting step in this mechanism. Accordingly, the ferric hydroperoxide intermediate has never been observed in wild-type peroxidases.

Cyanide binds ferric heme iron strongly and forms stable ferric cyanide complexes for all peroxidases (*4*). X-ray crystal structures of the ferric cyanide complexes of peroxidases showed that two of the water molecules in the distal heme pocket are replaced on cyanide coordination and that heme-bound cyanide forms strong hydrogen bonds with distal His and Arg, as proposed for hydrogen peroxide (Figure 1) (*8*−*10*). The ferric cyanide complex is thus a good model of the ferric hydroperoxide intermediate of peroxidase, not only in binding mode but also in size and charge. The ferric cyanide complex would be exposed to the same push and pull effects as the ferric hydroperoxide intermediate on its way to compound I, and thus the push and pull effects for the heme-bound cyanide would be directly related to the O−O bond cleavage step.

Recently, we succeeded in the first detection of paramagnetic ^{13}C NMR[1] signals of the heme-bound cyanides of ferric heme

[†]This work was supported by grants from CREST, Japan Science and Technology Agency, and the Global COE Program, the Japan Science Promotion Society (H.F.).

*To whom correspondence should be addressed. E-mail: hiro@ims.ac.jp. Telephone: +81-564-59-5578. Fax: +81-564-59-5600.

[1]Abbreviations: NMR, nuclear magnetic resonance; EPR, electron paramagnetic resonance; TMS, tetramethylsilane; CcP, cytochrome *c* peroxidase; CIP, *C. cinereus* peroxidase; ARP, *A. ramosus* peroxidase; Prx, peroxidase; wt, wild-type; PDB, Protein Data Bank.

Published on Web 12/02/2009

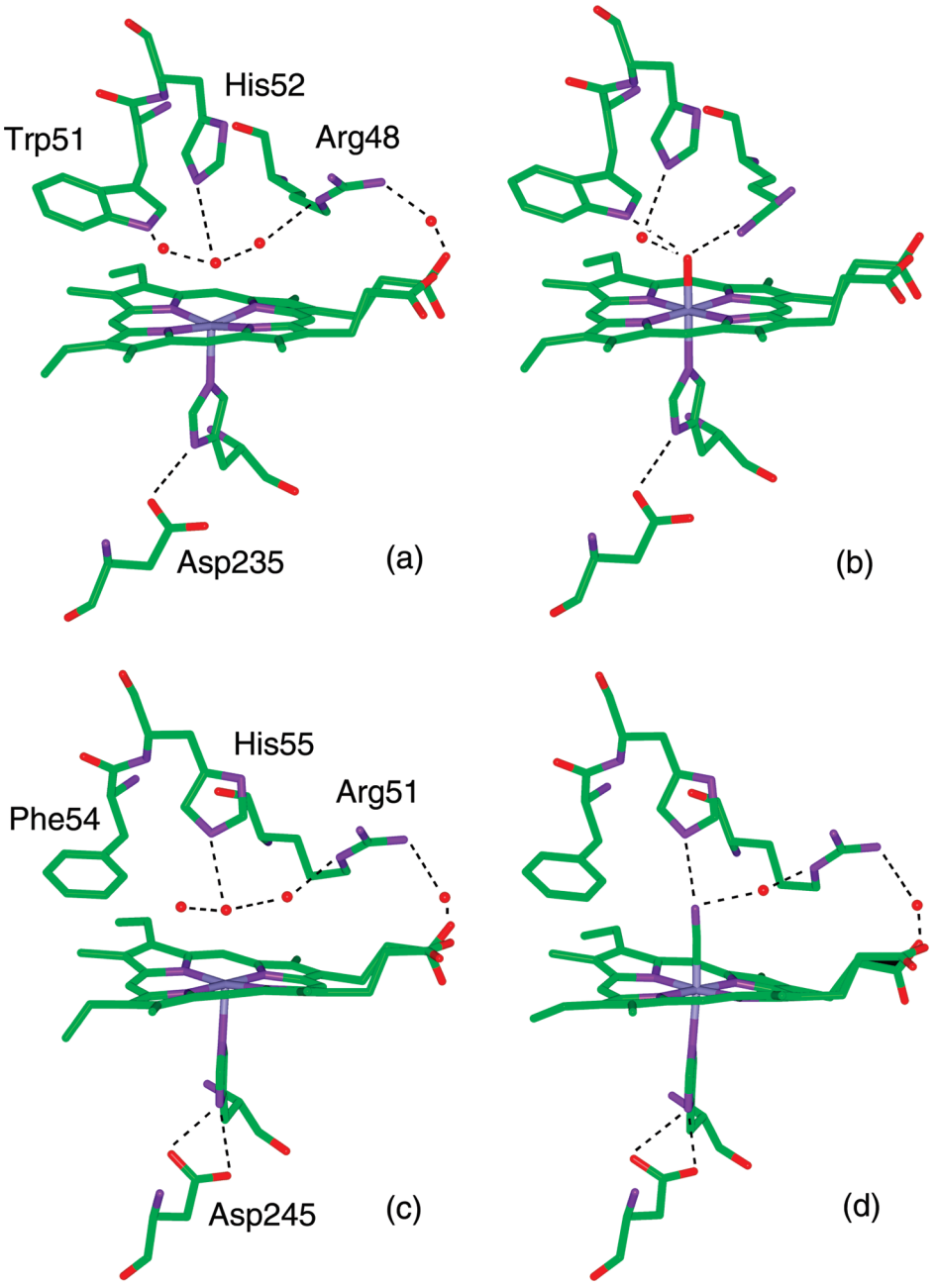

FIGURE 1: Active site structures of (a) cytochrome *c* peroxidase (CcP), (b) CcP compound I, (c) *Coprinus cinereus* peroxidase (CIP), and (d) the CIP cyanide complex, created from the coordinates obtained from PDB entries 1ZBY, 1ZBZ, 1ARP, and 2E39, respectively.

complexes and heme proteins and showed that the ^{13}C and ^{15}N NMR spectroscopy of heme-bound cyanide is a sensitive tool for monitoring the push and pull effects in the active sites of heme proteins (*11*−*13*). Via this spectroscopy, we demonstrated that the push and pull effects of wild-type peroxidases are much stronger than those of other heme proteins (*14*). Moreover, the push effect is linearly correlated to the rate of compound I formation (*14*). Here, we conducted ^{13}C and ^{15}N NMR spectroscopy of ferric cytochrome *c* peroxidase (CcP) and *Coprinus cinereus* peroxidase (CIP) mutants to study functional roles of conserved amino acids around heme in the push and pull effects. CcP is a class I peroxidase and has been extensively studied for several decades (*1*). CIP belongs to family of class II peroxidases and is also known as *Arthromyces ramosus* peroxidase (ARP) (*1*). CcP and CIP have quite similar active site structures (Figure 1), but different compound I formation rates (*15*−*18*). Roles of the distal His and Arg, the proximal Asp, and the distal Trp or Phe in the push and pull effects were studied using the following mutants, Arg48Leu, His52Leu, Arg48Leu/His52Leu, Trp51Phe, Asp235Asn, and Asp235Ala for CcP and Arg51Leu, Arg51Lys, Arg51Asn, Phe54Trp, and Asp245Ile for CIP (Figure S1 of the Supporting Information). In combination with the crystal structures and compound I formation rates of these mutants, the functional roles of these amino acids are discussed.

MATERIALS AND METHODS

Chemicals. Stable isotope-labeled potassium cyanide ($K^{13}C^{15}N$, >99%) was purchased from ISOTEC Inc. (Miamisburg, OH). All other chemicals were of reagent grade. Solutions were prepared using Milli-Q water (Millipore) or D_2O (Cambridge Isotope Laboratories, Inc.).

Enzyme Preparation. Wild-type CIP (wtCIP) and its mutants were expressed in *Aspergillus oryzae* and purified as described elsewhere (*19*, *20*). CIP enzymes were stored as ammonium

Table 1: ^{13}C and ^{15}N NMR Shifts of the Heme-Bound $^{13}C^{15}N$ of CcP and CIP at 298 K

		^{13}C NMR (ppm from TMS)		^{15}N NMR (ppm from $^{15}NO_3^-$)				
enzyme	pH(D)	observed	contact shift	observed	contact shift	$^{15}N/^{13}C$[a]	k_1 (M^{-1} s^{-1})	ref
				Cytochrome *c* Peroxidase				
wild type	7.2	−3501	−3944	605	645	0.164	4.5×10^7	*17*
His52Leu	7.2	−3542	−3985	660	700	0.176	7.3×10^2	*32*
				687	727	0.182		
Arg48Leu	5.3			565	605		8.2×10^5	*27*
	6.8			554	594			
His52Leu/Arg48Leu	6.8			730	770			
Trp51Phe	6.9	−3594	−4037	595	635	0.157	2.2×10^7	*33*
Asp235Asn	6.8	−3652	−4221	699	705	0.167	9.4×10^6	*38*
Asp235Ala	6.7	−3722	−4291	684	690	0.161		
				C. cinereus Peroxidase				
wild type	7.4	−3699	−4178	578	609	0.146	9.9×10^6	*18*
Arg51Asn	7.5	−3710	−4192	584	615	0.147	9.9×10^5	*24*
Arg51Lys	5.3	−3718	−4200	589	620	0.148		
	7.4			589	620			
	8.3	−3711	−4193	588	619	0.148	8.6×10^5	*24*
				627	658	0.157		
				661	692	0.165		
Arg51Leu	7.5	−3768	−4250	572	603	0.142	9.3×10^4	*24*
Phe54Trp	7.3	−3543	−4025	585	616	0.153	6.6×10^6	[b]
Asp245Ile	7.7	−3801	−4370	660	666	0.152	7.7×10^6	[c]

[a]The ratios are absolute values. [b]Welinder, K. G., et al., unpublished results. [c]The k_1 for CIP Asp245Ile is a preliminary value (Welinder, K. G., unpublished results).

sulfate precipitates at 4 °C. The wild-type CcP (wtCcP) gene was amplified from genomic DNA isolated from *Saccharomyces cerevisiae* strain W303-1B and subcloned into pET-20b (Novagen). The QuikChange mutagenesis method (Stratagene) was used for site-directed mutagenesis. DNA sequences of wild-type CcP (wtCcP) and its variants were confirmed by sequencing (CEQ8000, Beckman-coulter; ABI PRISM AVANT, Applied Biosystems). The enzymes were heterologously expressed in *Escherichia coli* BL21(DE3) and purified according to the method of Teske et al. (*21*). After DEAE Fast Flow anion exchange chromatography and Sephacryl-200 gel filtration (both GE Healthcare), enzymes were crystallized by dialysis against deionized water at 0 °C. The resulting crystals were stored as a water suspension at −80 °C until they were measured.

Paramagnetic NMR Analyses. ^1H, ^{13}C, and ^{15}N NMR spectra of peroxidases were obtained on a JEOL Lambda-500 spectrometer. The enzyme samples were prepared using 100 mM potassium phosphate buffer (pH 6.8−7.0) in D_2O and concentrated to 2−4 mM using an Amicon Ultra-15 apparatus (Millipore). After concentration, an excess amount of isotope-labeled cyanide was added. The pH(D) values of NMR samples were measured with a Horiba F-22 pH meter as summarized in Table 1. ^{13}C NMR spectra were recorded at sweep widths of 200 kHz at 125.27 MHz using 4K data points. ^{15}N NMR spectra were recorded at sweep widths of 100 kHz at 50.73 MHz using 4K data points. The pulse repetition time and pulse width were 0.075 s and 8 μs, respectively. Typically, 500000 transients were collected for both ^{13}C and ^{15}N NMR measurements. The chemical shift values of the ^{13}C and ^{15}N NMR spectra were referenced to external tetramethylsilane (TMS) in chloroform and sodium nitrate ($Na^{15}NO_3$) in deuterium oxide, respectively. Downfield and upfield indicate low-frequency and high-frequency regions, and left and right sides in an NMR spectrum, respectively. Analyses of NMR paramagnetic shifts were conducted as described previously (*12*, *14*). The diamagnetic shifts of ^{13}C and ^{15}N NMR signals of heme-bound cyanide could be estimated from the ^{13}C and ^{15}N NMR shifts of diamagnetic potassium ferrocyanide [$K_4Fe(CN)_6$], ^{13}C at 177 ppm from TMS and ^{15}N at −111 ppm from $^{15}NO_3^-$. For the heme-bound cyanide of proximal Asp mutants of CcP and CIP, the ^{13}C and ^{15}N dipolar shifts were calculated to be 392 and 105 ppm with EPR g values of 3.39, 1.94, and 1.17, r_{Fe-C} = 1.99 Å, and r_{Fe-N} = 3.09 Å, respectively (*12*, *22*). For the other cyanide−peroxidase complexes, the ^{13}C and ^{15}N dipolar shifts for CcP and its mutants were calculated to be 266 and 71 ppm with EPR g values of 3.0, 2.1, and 1.2, r_{Fe-C} = 1.99 Å, and r_{Fe-N} = 3.09 Å, and for CIP and its mutants 305 and 80 ppm with EPR g values of 3.09, 2.13, and 1.17, r_{Fe-C} = 1.96 Å, and r_{Fe-N} = 3.04 Å (*11*). The contact shifts of the ^{13}C and ^{15}N NMR signals were calculated by the following equation: contact shift (ppm) = observed shift − diamagnetic shift − dipolar shift.

RESULTS AND DISCUSSION

^{13}C and ^{15}N NMR Spectroscopy. Because of the paramagnetic effect of the ferric heme iron, the ^{13}C and ^{15}N NMR signals of heme-bound cyanide ($^{13}C^{15}N$) show extremely large upfield shifts (−3500 to −4100 ppm) and large downfield shifts (500−1100 ppm) (*11*, *12*). These upfield and downfield paramagnetic shifts correlate linearly to electron spin densities on the ^{13}C and ^{15}N atoms, respectively. When the push effect of proximal His is increased with an increase in the extent of the hydrogen bonding interaction of the proximal Asp, the binding of cyanide becomes weaker due to the trans effect. This results in a less effective electron spin transfer from heme iron to the heme-bound cyanide (Figure 2). Therefore, an increased push effect will decrease the ^{13}C and ^{15}N NMR paramagnetic shifts. Hence, the

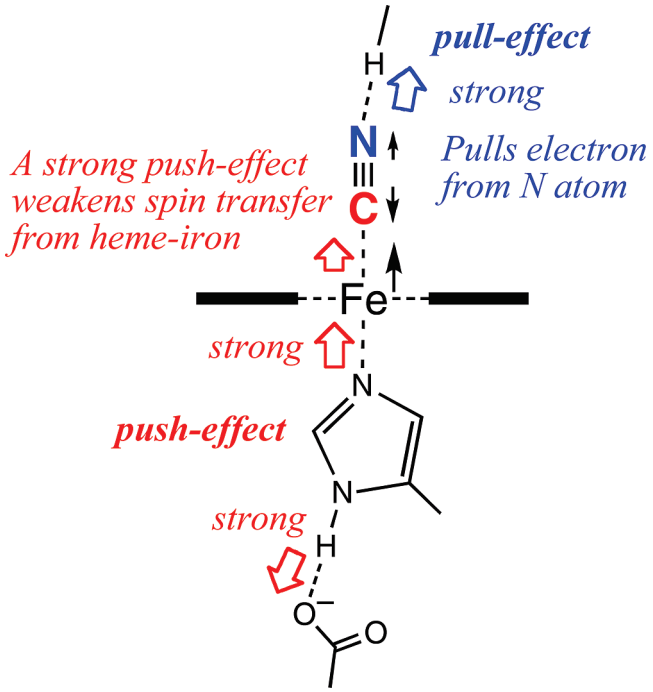

FIGURE 2: Change in the electron spin density on the C and N atoms of heme-bound cyanide induced by the push and pull effects. Low-spin ferric iron spin polarizes the negative spin on the C atom and the positive spin on the N atom (see the filled black arrows). This results in an extremely large downfield shift of the ^{13}C NMR signal, and a large downfield shift of the ^{15}N NMR signal: push effect (red) and pull effect (blue). The bold black lines denote a porphyrin plane.

^{13}C NMR signal moves downfield (left in an NMR spectrum), and the ^{15}N NMR signal moves upfield (right in an NMR spectrum). In contrast, the pull effect pulls the electrons more strongly away from the ^{15}N atom than from the ^{13}C atom (Figure 2). Therefore, with an increase in the pull effect, the ^{15}N NMR paramagnetic shift decreases, i.e., moves upfield, while the ^{13}C NMR paramagnetic shift decreases just slightly. The ratio of the ^{13}C and ^{15}N NMR shifts is changed by the pull effect. However, the ratio of the ^{13}C and ^{15}N NMR shifts remains almost constant despite changes in the push effect from the proximal His, because the electron spin polarization ratio from the ^{13}C atom to the ^{15}N atom is not changed by the push effect. For these reasons, the ^{13}C NMR signal is a good measure of the push effect, and the ratio (absolute value) of the ^{15}N NMR shift over the ^{13}C NMR shift is a good measure of the pull effect. To be correct, the contact shift rather than the observed shift was used for calculating the ratio.

^{13}C and ^{15}N NMR Spectra of a Distal His Mutant. Distal His in peroxidases has been shown to function as a base catalyst accepting a proton from the hydrogen peroxide substrate on its binding to heme iron, and as an acid catalyst on release of water during compound I formation (*5*). To study the pull effect from distal His, we measured ^{13}C and ^{15}N NMR spectra for CcP His52Leu bound to $^{13}C^{15}N$ (Figure 3 and Table 1). The ^{13}C NMR signal is observed at −3542 ppm for CcP His52Leu (Figure 3a). This is a slight upfield shift (~1%) compared to the signal of wild-type CcP (wtCcP) at −3501 ppm (*13*). The ^{15}N NMR spectrum for CcP His52Leu shows two signals at 660 and 687 ppm (Figure 3b), which were significantly downfield (~10%) of the wtCcP signal at 605 ppm (*13*). The ratios of the ^{15}N NMR contact shift over the ^{13}C NMR contact shift ($^{15}N/^{13}C$) for His52Leu (0.176 and 0.182) were larger than for wtCcP (0.164), and far outside the range for the ratios of wild-type peroxidases

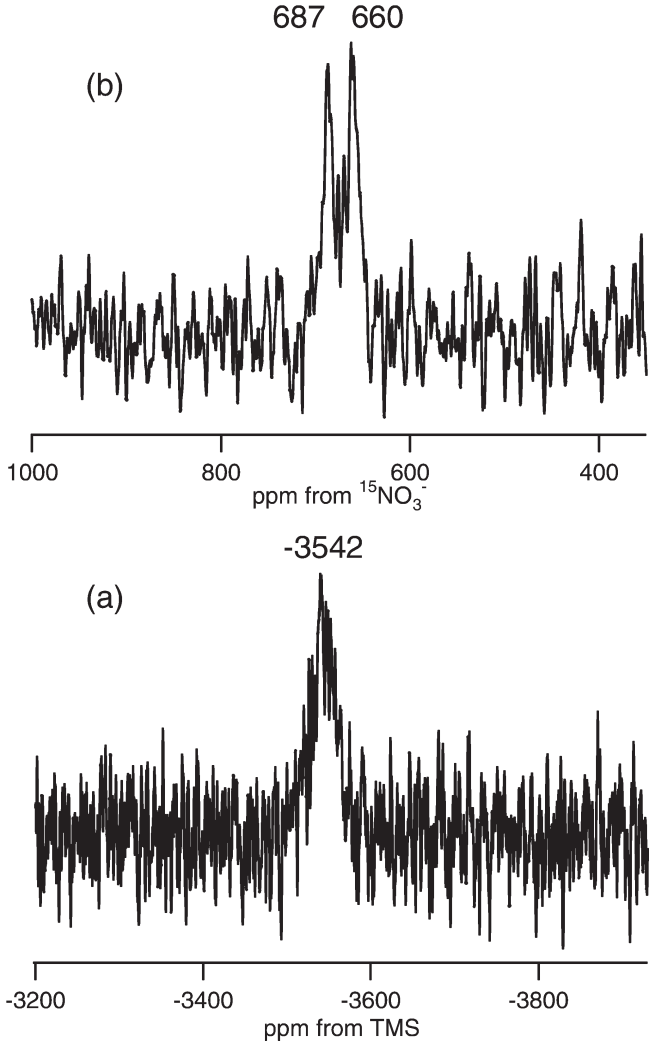

FIGURE 3: (a) ^{13}C and (b) ^{15}N NMR spectra of heme-bound $^{13}C^{15}N$ of ferric CcP His52Leu in 100 mM potassium phosphate [pH(D) 7.2] at 298 K.

(0.145−0.164), but still smaller than those of other wild-type heme proteins (>0.19) (*14*). Since the $^{15}N/^{13}C$ ratio increases with a decrease in the pull effect, this indicates that the hydrogen bonding interaction with the heme-bound cyanide is significantly weakened by the mutation of the distal His to Leu. The push effect is not changed by the distal His mutation. The slight upfield shift of the ^{13}C NMR signal can be explained by the loss of hydrogen bonding interaction with the heme-bound cyanide because the ^{13}C NMR signal showed a small upfield shift (~50 ppm) in the absence of a hydrogen bonding donor, methanol, in a previous model study (*12*). All of the ^{13}C and ^{15}N NMR results presented here thus support the view that distal His is an essential proton donor to heme-bound hydroperoxide. The two ^{15}N NMR signals indicate that heme-bound cyanide of His52Leu contains at least two distinct coordination structures. This is in agreement with a previous ^{1}H NMR study of CcP His52Leu, which showed the presence of two dominant species in dynamic equilibrium (Figure S2 of the Supporting Information) (*23*). Arg48 and Trp51 are likely hydrogen bond donors in the heme pocket of CcP His52Leu (Figure S1 of the Supporting Information). Two positions of the distal Arg48 of wtCcP have been demonstrated by crystallographic studies (*6*, *8*). Similarly, it appears that the flexible Arg side chain forms different hydrogen bonding interactions with the heme-bound

cyanide, resulting in two distinct conformations in the heme pocket. The hydrogen bonding interaction of the heme-bound cyanide with Arg in CcP His52Leu is further confirmed by a distal His and Arg double mutant (see below).

^{13}C and ^{15}N NMR Spectra of the Distal His and Arg Double Mutant. The hydrogen bonding interactions from the distal His and Arg were analyzed further in the CcP Arg48Leu/His52Leu double mutant (Table 1). The ^{15}N NMR shift of CcP Arg48Leu/His52Leu at 730 ppm was much larger than for the His52Leu mutant, but similar to that (733 ppm) of the peroxidase model complex formed by imidazolate, cyanide, and hemin dimethyl ester in dichloromethane (*12*). This suggests a very hydrophobic environment of the distal heme pocket of CcP Arg48Leu/His52Leu. The downfield shift of the ^{15}N NMR signal in the order wtCcP < His52Leu < Arg48Leu/His52Leu confirms that both distal His and Arg contribute to the strong pull effect in wtCcP. We could not detect the ^{13}C NMR signal of the heme-bound $^{13}C^{15}N$ of ferric CcP Arg48Leu/His52Leu, probably due to fluctuation of the heme pocket in this mutant. The loss of the hydrogen bonds with the Arg48Leu/His52Leu mutations would increase the mobility of the distal heme pocket and lead to rapid exchange between multiple species with different ^{13}C NMR shifts, resulting in broadening of the ^{13}C NMR signal. The fluctuation of the heme pocket is further confirmed by significant broadening of ^{1}H NMR signals of the heme methyl protons of CcP Arg48Leu/His52Leu (Figure S2 of the Supporting Information). Therefore, the $^{15}N/^{13}C$ ratio could not be determined for CcP Arg48Leu/His52Leu.

^{13}C and ^{15}N NMR Spectra of the Distal Arg Mutants. In crystal structures of ferric cyanide complexes of peroxidases, the distal Arg engages in hydrogen bonding interaction with the heme-bound cyanide via a water molecule (Figure 1d) (*8*−*10*). To study the functional role of the distal Arg residue, we measured ^{13}C and ^{15}N NMR spectra for the distal Arg mutants of CIP, Arg51Leu, Arg51Asn, and Arg48Lys, and also Arg48Leu for CcP (Table 1). The ^{13}C and ^{15}N NMR shifts of CIP Arg51Asn were similar to those of wild-type CIP (wtCIP). The replacement of the charged distal Arg with the neutral, but polar Asn, did not change the push and pull effects. These results also suggest that the contribution of the cationic character of the distal Arg to the pull effect is rather small, in agreement with a previous study (*24*). As the side chain of Asn is shorter than that of the original Arg, rearrangements of the hydrogen bonding network, including repositioning of water molecules in the heme pocket, are likely to occur, compensating for the loss of the hydrogen bonding interaction from distal Arg.

The ^{13}C and ^{15}N NMR shifts of heme-bound $^{13}C^{15}N$ of CIP Arg51Lys at pH(D) 5.3 and 8.3 were also very close to those of wtCIP, indicating only a minor effect on the push and pull effects with the mutation. However, two additional ^{15}N NMR signals were detected at 627 and 661 ppm at pH(D) 8.3 (Figure 4). The pH-dependent ^{15}N NMR spectral change would reflect the protonation of distal Lys with a pK_a of 7.4−8.3. A previous ^{1}H NMR study of CIP Arg51Lys reported the pK_a of the Lys51 side chain to be ~5.2 (*24*, *25*). The hydrogen bonding interaction with the negatively charged heme-bound cyanide may stabilize the charged form of Lys51, leading to an increase in the pK_a value by at least 2 pH units. Since the ^{15}N NMR signal shifts downfield with a loss of hydrogen bonding interaction, the ^{15}N NMR signals at 627 and 661 ppm indicate weak or negligible interactions between the heme-bound cyanide and the deprotonated form of Lys51.

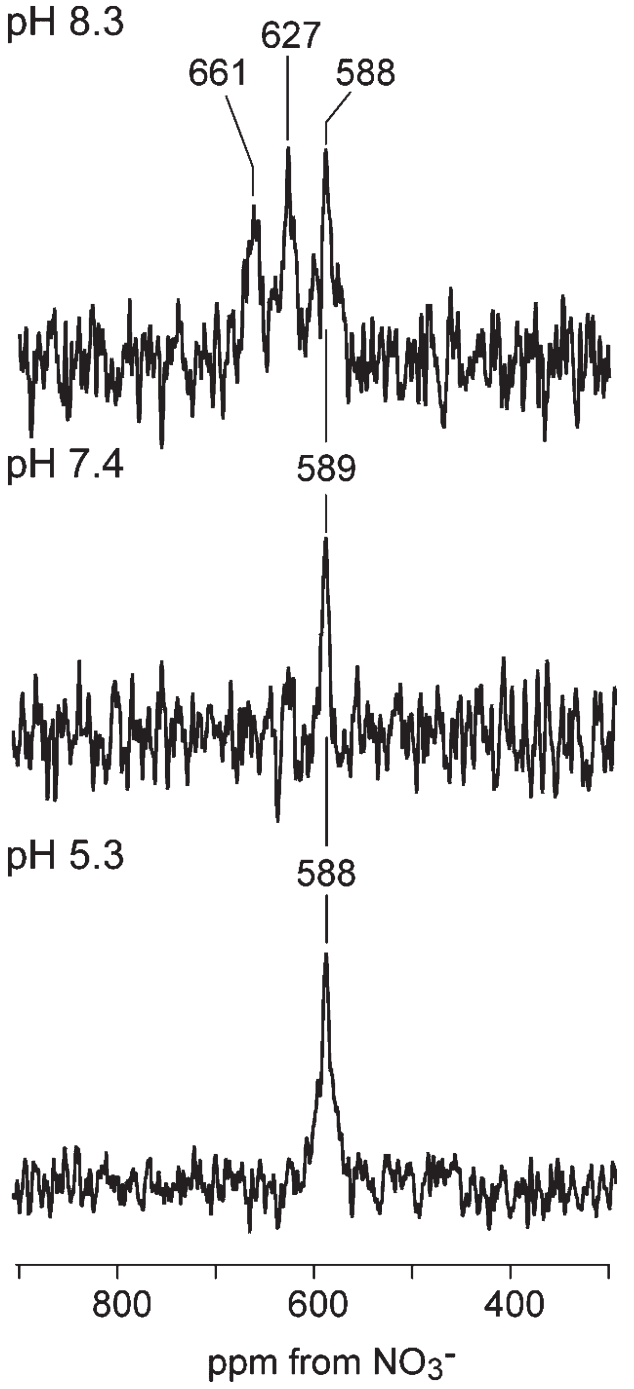

FIGURE 4: ^{15}N NMR spectra of heme-bound $^{13}C^{15}N$ of ferric CIP Arg51Lys at various pH values in 100 mM potassium phosphate at 298 K: pH(D) 5.3, 7.4, and 8.3.

In contrast to CIP Arg51Asn and Arg51Lys mutants, the mutation of the distal Arg to Leu showed structural changes at both the distal and proximal sides of heme. The ^{13}C NMR signal of CIP Arg51Leu showed a 69 ppm upfield shift compared to that of wtCIP (Table 1), clearly indicating a decrease in the push effect of the mutant. The weak push effect of CIP Arg51Leu was also suggested by previous resonance Raman and electronic absorption spectral studies (*24*, *25*). On the other hand, we could not identify the ^{13}C NMR signal of the heme-bound cyanide for CcP Arg48Leu, as for the CcP Arg48Leu/His52Leu double mutant. In general, CcP is less stable than CIP to increased temperature and basic pH values. Introduction of Leu at the position of Arg in CcP may induce a larger structural alteration in the heme pocket

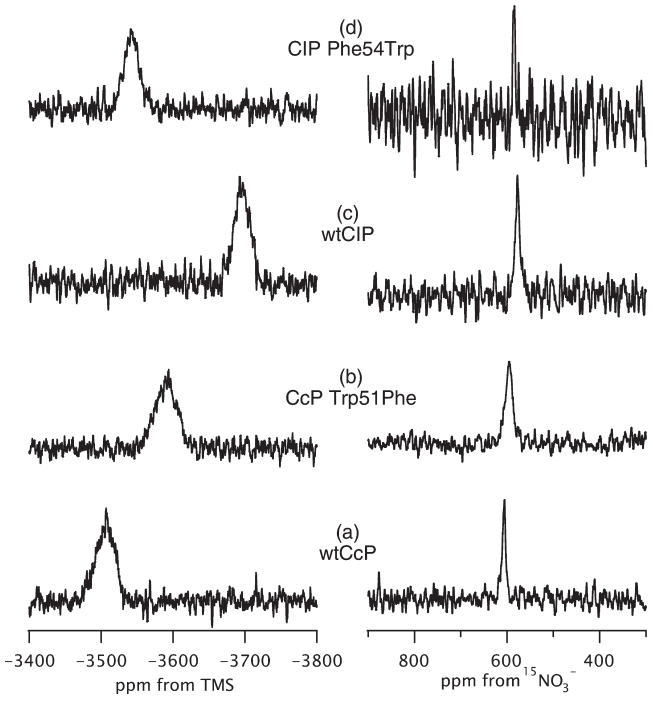

FIGURE 5: ^{13}C (left) and ^{15}N (right) NMR spectra of heme-bound $^{13}C^{15}N$ of ferric CcP Trp51Phe and CIP Phe54Trp in 100 mM potassium phosphate at 298 K: (a) wtCcP, (b) CcP Trp51Phe, (c) wtCIP, and (d) CIP Phe54Trp.

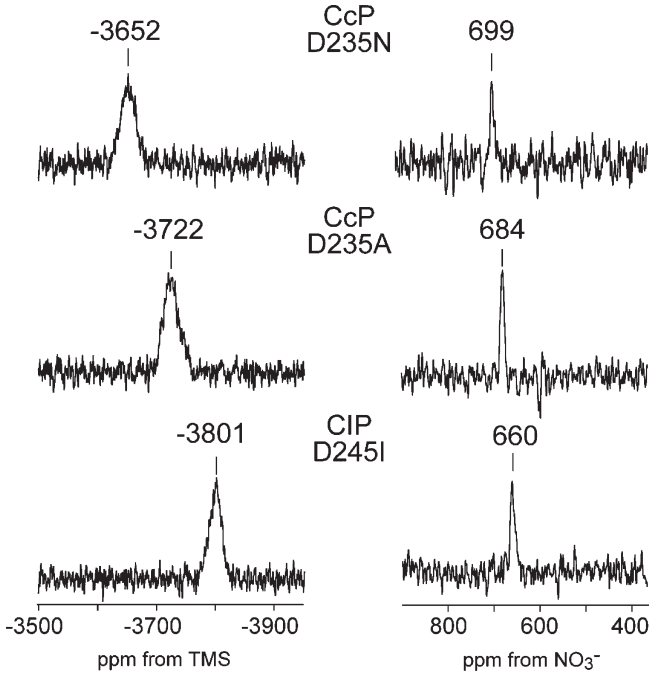

FIGURE 6: ^{13}C and ^{15}N NMR spectra of heme-bound $^{13}C^{15}N$ of proximal Asp mutants in 100 mM potassium phosphate at 298 K: CIP Asp245Ile, CcP Asp235Ala, and CcP Asp235Asn.

than in CIP, resulting in extreme broadening of the ^{13}C NMR signal due to multiple species with different strengths of the proximal push effect. In fact, broadening of ^1H NMR signals for the heme methyl protons was observed for CcP Arg48Leu and Arg48Leu/His52Leu, but not for CIP Arg51Leu (Figures S2 and S3 of the Supporting Information). Similarly, the ^{15}N NMR upfield shifts of 40−50 ppm for CcP Arg48Leu are larger than the 6 ppm shift for CIP Arg51Leu. As suggested by the upfield shifts of the ^{15}N NMR signals, the $^{15}N/^{13}C$ ratio indicates that the hydrogen bonding interaction between distal His and heme-bound cyanide would be strengthened by this mutation. The distal Arg forms hydrogen bonds with protein backbone carbonyls and a water molecule and assists in maintaining the active site structure (*15*, *16*). Therefore, the loss of the hydrogen bonds of the distal Arg would increase the mobility of distal His and allow it to move close to heme-bound cyanide and to form a stronger hydrogen bond with cyanide. This is consistent with previous reports on distal His of CcP Arg48Leu ($pK_a = 7.5 \pm 0.1$), which readily bound to heme forming a bis-His complex under basic conditions (*26*, *27*). All of these results clearly indicate that distal Arg is essential to maintaining the distal heme pocket structure via its hydrogen bonding interactions, which place distal His in the proper position to accept a proton from hydrogen peroxide.

^{13}C and ^{15}N NMR Spectra of CcP Trp51Phe and CIP Phe54Trp Mutants. Most plant peroxidase superfamily class I peroxidases, such as CcP, possess a distal Trp residue. Class II and III peroxidases, including CIP, have a Phe residue at this position (Figure 1). The functional roles of these aromatic residues were studied in CcP Trp51Phe and CIP Phe54Trp. Figure 5 compares the paramagnetic ^{13}C and ^{15}N NMR spectra of the heme-bound $^{13}C^{15}N$ of ferric cyanide complexes of these mutants and the wild types. The ^{13}C NMR signal of CIP Phe54Trp was observed at −3543 ppm, which is far downfield (∼150 ppm) from the shift for wtCIP, but close to that for wtCcP. On the other hand, the ^{13}C NMR signal of CcP Trp51Phe showed an opposite large upfield shift (∼90 ppm), close to the shift of wtCIP. In contrast, the ^{15}N NMR shifts of CcP Trp51Phe and CIP Phe54Trp did not show drastic changes compared to those of the wild-type peroxidases (Figure 5 and Table 1). Therefore, the $^{15}N/^{13}C$ ratio (0.157) for CcP Trp51Phe is smaller than that (0.164) for wtCcP and shifts to that (0.146) of wtCIP, while the ratio (0.153) for CIP Phe54Trp is larger than that for wtCIP and shifts to the ratio of wtCcP (Figure S4 of the Supporting Information). These results clearly show that the Trp and Phe modulate the push and pull effects. It appears that the smaller Phe residue provides more space and flexibility in the distal heme pocket, leading to looser binding of the proximal His to the heme iron and the distal His to cyanide than Trp.

In our previous report (*14*), we showed that class I peroxidases possess a stronger push effect than class II peroxidases. We proposed that this was caused by differential rotation of the imidazole plane of the proximal His relative to a N−Fe−N line in the heme plane; the parallel orientation gives a stronger electronic interaction between the proximal His and heme (stronger push effect), contrary to the staggered orientation (weaker push effect) (Figure 6 of ref *14*). The results presented here indicate that the steric effect of the amino acid at the position of the distal Trp in class I peroxidases and the distal Phe in class II and III peroxidases is another factor controlling the push and pull effects.

^{13}C and ^{15}N NMR Spectra of the Proximal Asp Mutants. The proximal Asp side chain is hydrogen-bonded to the Nδ1 atom of the proximal His (Figure 1). This interaction increases the imidazolate character and the push effect of proximal His. To investigate this hydrogen bonding effect, we recorded the ^{13}C and ^{15}N NMR spectra of the heme-bound $^{13}C^{15}N$ of CcP Asp235Asn and Asp235Ala mutants (Figure 6). As shown in Figure 6 and Table 1, the mutations of the proximal Asp dramatically affected both the ^{13}C and ^{15}N NMR shifts.

The ^{13}C NMR signals of the Asn and Ala mutants were 151 and 221 ppm upfield, respectively, relative to those of wtCcP. Thus, the push effect of the proximal His increases in the following order: Asp235Ala < Asp235Asn < wtCcP. This is consistent with previous studies of these mutants (*26*, *28*). In the crystal structure of CcP Asp235Asn, the Oδ1 atom of Asn interacts with the proximal His Nδ1 atom at a distance of 2.98 Å (*15*), whereas the proximal His Nδ1 atom of CcP Asp235Ala did not form any interaction (*28*). Similarly, the ^{13}C NMR signal of CIP Asp245Ile was detected at −3801 ppm from TMS, which is 102 ppm upfield relative to that of wtCIP (Figure 6 and Table 1). All of these results clearly show that the strong hydrogen bond between proximal Asp and His in peroxidase increases the push effect.

It is noteworthy that the push effect, even in apolar proximal Asp mutants of peroxidases, is stronger than in other heme proteins, such as myoglobin, hemoglobin, and cytochrome *c*. For example, the ^{13}C NMR shift of sperm whale myoglobin was found at −4145 ppm, which is much further upfield than those of the proximal Asp mutants of peroxidases (*11*). Therefore, in peroxidases, the push effect of the proximal His is intrinsically stronger than in other heme proteins. This may be due to the differential locations of the helix containing proximal His in peroxidases and globins, as observed by Poulos (*29*). The proximal helix in globins is more directly under the heme but farther from the heme plane than in peroxidases (Figure S5 of the Supporting Information), which would make the proximal environment more rigid and the push effect stronger in peroxidases.

The ^{15}N NMR signals of CcP Asp235Asn and Asp235Ala were observed at 699 and 684 ppm from $^{15}NO_3^-$, respectively (Figure 6 and Table 1). The electron spin transfer to the heme-bound cyanide becomes more effective with these mutations due to the weaker push effects (Figure 2). The $^{15}N/^{13}C$ ratios of 0.167 and 0.161 for CcP Asp235Asn and Asp235Ala, respectively, were close to the value of 0.164 for wtCcP, indicating no significant change in the pull effect. The ^{15}N NMR signal of CIP Asp245Ile was observed at 660 ppm, giving a $^{15}N/^{13}C$ ratio of 0.152 similar to that of wtCIP. In conclusion, the proximal Asp−His hydrogen bond does not affect the pull effect of the distal side.

Functional Roles of Active Site Amino Acids in Compound I Formation. Figure 7 shows the correlation of the push effect (^{13}C NMR shift) with the logarithm of the rate constant of compound I formation. Interestingly, the proximal Asp mutants (colored red) are close to the correlation line for wild-type peroxidases (colored black). This confirms our previous finding that the push effect is the major contributor to the rates of compound I formation of wild-type peroxidases (*14*). But how does the push effect modulate the rate of compound I formation? The rate-limiting step of compound I formation is the binding step of hydrogen peroxide, which includes reorganization of the distal heme pocket with water replacement and the uptake of a proton by the distal His. With a decrease in the push effect, the electron density on the heme iron decreases, and the interaction of the heme iron with water in the distal pocket becomes stronger (*15*, *22*, *26*, *28*, *30*). Therefore, with a decrease in the push effect, more energy is required for replacement of heme-bound water with hydrogen peroxide, increasing the transition state free energy and slowing the rate of formation of compound I.

The distal mutants exhibited a large deviation from the correlation line, suggesting participation of other factors caused by the distal mutations in the compound I formation process.

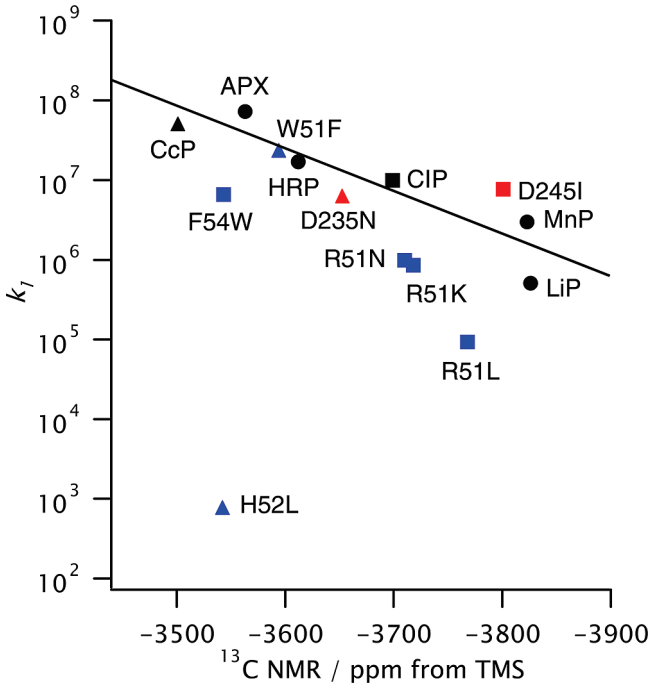

FIGURE 7: Semilogarithmic plot of compound I formation rate constants vs ^{13}C NMR chemical shifts of various peroxidases. The black, red, and blue points are data for wild-type peroxidases, proximal mutants, and distal mutants, respectively. The squares, triangles, and circles depict data for CIP, CcP, and other peroxidases, respectively.

The $^{15}N/^{13}C$ ratios (0.176 and 0.182) for CcP His52Leu were much increased, indicating that distal His is the key amino acid residue creating the pull effect. However, the $^{15}N/^{13}C$ ratios were still lower than those (> 0.19) of other heme proteins, probably due to new hydrogen bonding interactions from distal Arg. Therefore, compound I was still formed very slowly even in the absence of distal His (*31*, *32*). Thus, the initial reorganization of the distal pocket structure of CcP His52Leu and the lack of base catalysis lead to the very slow formation of compound I.

The compound I formation rates of CIP Arg51Asn and Arg51Lys were decreased to $\sim^1/_{10}$ of that of wtCIP (Table 1) (*24*). Because the push and pull effects were unchanged, the coordination of hydrogen peroxide would be slowed by the mutations. Previous spectroscopic studies of these mutants have shown that a water molecule or the Lys side chain was coordinated to the heme in the resting state (*25*). Moreover, the X-ray crystal structure of CcP Arg48Lys showed changes in the hydrogen bonding network in the distal heme pocket and a slight shift of the Lys48 side chain (*27*). These changes will increase the required energy of reorganization of the distal heme pocket and decrease the rate of formation of compound I. A much more drastic decrease in the rate of formation of compound I was reported for CIP Arg51Leu. The decrease in the push effect and the increase in the pull effect suggested drastic changes in the structure in the heme pocket. The X-ray crystal structure and spectroscopic studies of the distal Arg mutants replaced with Leu indicated a loss of water molecules at the proximal site because of the hydrophobic Leu (*27*). The Leu side chain may hinder incoming hydrogen peroxide, resulting in very slow binding.

This study showed that the distal Trp in CcP and Phe in CIP modulated the push and pull effects but were not essential in controlling the rate of formation of compound I. The rate of formation of compound I of CcP is 5-fold faster than that of CIP.

However, the rate of formation of compound I of CIP did not increase even when the structure of the distal heme pocket became more like CcP via the mutation of the distal Phe to Trp. The distal heme pockets of CcP and CIP might be well organized, and the mutation of the aromatic amino acid might result in an increase in reorganization energy, leading to a decrease in the rate of formation of compound I (*33*, *34*). On the other hand, a drastic change in the push and pull effects of these mutants would change the reactivity of the ferric hydroperoxide intermediate, as well as compound I, which can be ascribed to the reactivity of distal Trp mutants (*35*−*37*).

CONCLUSION

Paramagnetic ^{13}C and ^{15}N NMR spectroscopy of heme-bound cyanide in ferric peroxidase mutants allowed us to study the contributions of conserved amino acids around heme in the pull and push effects. Analyses of paramagnetic shifts of heme-bound cyanide ^{13}C and ^{15}N atoms showed that the pull effect on the distal side is mainly due to distal His, while the push effect induced by proximal His is drastically enhanced by the hydrogen bonding interaction with proximal Asp. The distal Arg seems to be involved in compound I formation indirectly; however essential it is in sustaining the distal heme pocket and its hydrogen bonding interactions. The distal Trp or Phe plays a structural role that affects the push and pull effects. The push effect correlated with the rate constant of compound I formation in wild-type peroxidases (Figure 7). The push effect modulates not only the rate of heterolytic cleavage of the O−O bond but also the removal of water or other ligands bound at the sixth coordination position of the heme iron prior to hydroperoxide binding in compound I formation. The hindrance of hydrogen peroxide diffusion and reorganization of a distorted heme pocket also contribute to the rate of compound I formation. The degree of deviation from the correlation line might thus be a measure of structural distortion (hydrogen bonding network, partial collapse, and steric hindrance) of the heme pocket in the peroxidase enzyme.

SUPPORTING INFORMATION AVAILABLE

Active site view of CcP mutants, ^{1}H NMR spectra of CcP mutants, ^{1}H NMR spectra of CIP mutants, correlation diagram of the push and pull effects for CcP and CIP mutants, and comparison between the location of the proximal helix and His in myoglobin and wtCcP. This material is available free of charge via the Internet at http://pubs.acs.org.

REFERENCES

1. Welinder, K. G. (1992) Superfamily of plant, fungal and bacterial peroxidases. *Curr. Opin. Struct. Biol. 2*, 388–393.
2. Poulos, T. L. (1987) Heme enzyme crystal structures. *Adv. Inorg. Biochem. 7*, 1–36.
3. Dawson, J. H. (1988) Probing structure-function relations in heme-containing oxygenases and preoxidases. *Science 240*, 433–439.
4. Dunford, H. B. (1999) Heme Peroxidases , John Wiley and Sons, New York.
5. Poulos, T. L., and Kraut, J. (1980) The stereochemistry of peroxidase catalysis. *J. Biol. Chem. 255*, 8199–8205.
6. Bonagura, C. A., Bhaskar, B., Shimizu, H., Li, H., Sundaramoorthy, M., McRee, D. E., Goodin, D. B., and Poulos, T. L. (2003) High-resolution crystal structures and spectroscopy of native and compound I cytochrome c peroxidase. *Biochemistry 42*, 5600–5608.
7. Balny, C., Travers, F., Barman, T., and Douzou, P. (1987) Thermodynamics of the two step formation of horseradish peroxidase compound I. *Eur. Biophys. J. 14*, 375–383.
8. Edwards, S. L., and Poulos, T. L. (1990) Ligand binding and structural perturbations in cytochrome *c* peroxidase. A crystallographic study. *J. Biol. Chem. 265*, 2588–2595.
9. Fukuyama, K., Kunishima, N., Amada, F., Kubota, T., and Matsubara, H. (1995) Crystal structures of cyanide- and triiodide-bound forms of *Arthromyces ramosus* peroxidase at different pH values. Perturbations of active site residues and their implication in enzyme catalysis. *J. Biol. Chem. 270*, 21884–21892.
10. Badyal, S. K., Joyce, M. G., Sharp, K. H., Seward, H. E., Mewies, M., Basran, J., Macdonald, I. K., Moody, P. C. E., and Raven, E. L. (2006) Conformational mobility in the active site of a heme peroxidase. *J. Biol. Chem. 281*, 24512–24520.
11. Fujii, H. (2002) ^{13}C NMR signal detection of iron-bound cyanide ions in ferric cyanide complexes of heme proteins. *J. Am. Chem. Soc. 124*, 5936–5937.
12. Fujii, H., and Yoshida, T. (2006) ^{13}C and ^{15}N NMR studies of iron-bound cyanides of heme proteins and related model complexes: Sensitive probe for detecting hydrogen-bonding interactions at the proximal and distal sides. *Inorg. Chem. 45*, 6816–6827.
13. Tanaka, A., Nakamura, H., Shiro, Y., and Fujii, H. (2006) Roles of the heme distal residues of FixL in O_2 sensing: A single convergent structure of the heme moiety is relevant to the down-regulation of kinase activity. *Biochemistry 45*, 2515–2523.
14. Nonaka, D., Wariishi, H., and Fujii, H. (2009) Paramagnetic ^{13}C and ^{15}N NMR analyses of cyanide- ($^{13}C^{15}N$-) ligated ferric peroxidases: The push effect, not pull effect, modulates the compound I formation rate. *Biochemistry 48*, 898–905.
15. Wang, J., Mauro, M., Edwards, S., Oatley, S., Fishel, L., Ashford, V., Xuong, N., and Kraut, J. (1990) X-ray structures of recombinant yeast cytochrome *c* peroxidase and three heme-cleft mutants prepared by site-directed mutagenesis. *Biochemistry 29*, 7160–7173.
16. Kunishima, N., Fukuyama, K., Matsubara, H., Hatanaka, H., Shibano, Y., and Amachi, T. (1994) Crystal structure of the fungal peroxidase from *Arthromysus ramosus* at 1.9 Å resolution: Structural comparisons with the lignin and cytochrome c peroxidases. *J. Mol. Biol. 235*, 331–344.
17. Loo, S., and Erman, J. E. (1975) A kinetic study of the reaction between cytochrome c peroxidase and hydrogen peroxide. Dependence on the pH and ionic strength. *Biochemistry 14*, 3467–3470.
18. Abelskov, A., Smith, A., Rasmussen, C., Dunford, H., and Welinder, K. G. (1997) pH dependence and structural interpretation of the reactions of *Coprinus cinereus* peroxidase with hydrogen peroxide, ferulic acid, and 2,2′-azinobis(3-ethylbenzthiazoline-6-sulfonic acid). *Biochemistry 36*, 9453–9463.
19. Dalbøge, H., Jensen, E. B., and Welinder, K. G. (1998) U.S. Patent 5,744,323.
20. Tams, J., and Welinder, K. G. (1996) Unfolding and refolding of *Coprinus cinereus* peroxidase at high pH, in urea, and at high temperature. Effect of organic and ionic additives on these processes. *Biochemistry 35*, 7573–7579.
21. Teske, J., Savenkova, M., Mauro, J., Erman, J., and Satterlee, J. (2000) Yeast cytochrome *c* peroxidase expression in *Escherichia coli* and rapid isolation of various highly pure holoenzymes. *Protein Expression Purif. 19*, 139–147.
22. Ferrer, J. C., Turano, P., Banci, L., Bertini, I., Morris, I. K., Smith, K. M., Smith, M., and Mauk, G. (1994) Active site coordination chemistry of the cytochrome c peroxidase Asp235Ala variant: Spectroscopic and functional characterization. *Biochemistry 33*, 7819–7829.
23. Satterlee, J. D., Savenkova, M. I., Foshay, M., and Erman, J. E. (2003) Temperature, pH, and solvent isotope dependent properties of the active sites of resting-state and cyanide-ligated recombinant cytochrome *c* peroxidase (H52L) revealed by proton hyperfine resonance spectra. *Biochemistry 42*, 10772–10782.
24. Schiødt, C. B., Veitch, N. C., and Welinder, K. G. (2007) Roles of distal arginine in activity and stability of *Coprinus cinereus* peroxidase elucidated by kinetic and NMR analysis of the Arg51Gln, -Asn, -Leu, and -Lys mutants. *J. Inorg. Biochem. 101*, 336–347.
25. Neri, F., Indiani, C., Welinder, K. G., and Smulevich, G. (1998) Mutation of the distal arginine in *Coprinus cinereus* peroxidase: Structural implications. *Eur. J. Biochem. 251*, 830–838.
26. Smulevich, G., Mauro, J., Fishel, L., English, A., Kraut, J., and Spiro, T. (1988) Heme pocket interactions in cytochrome *c* peroxidase studied by site-directed mutagenesis and resonance Raman spectroscopy. *Biochemistry 27*, 5477–5485.
27. Vitello, L., Erman, J., Miller, M., Wang, J., and Kraut, J. (1993) Effect of arginine-48 replacement on the reaction between cytochrome *c* peroxidase and hydrogen peroxide. *Biochemistry 32*, 9807–9818.

28. Goodin, D., and McRee, D. (1993) The Asp-His-Fe triad of cytochrome *c* peroxidase controls the reduction potential, electronic structure, and coupling of the tryptophan free radical to the heme. *Biochemistry 32*, 3313–3324.
29. Poulos, T. L. (1996) The role of the proximal ligand in heme enzymes. *J. Biol. Inorg. Chem. 1*, 356–359.
30. Veitch, N. C., Gao, Y., and Welinder, K. G. (1996) The Asp245→Asn mutation of *Coprinus cinereus* peroxidase. Characterization by ^{1}H-NMR spectroscopy and comparison with the wild-type enzyme. *Biochemistry 35*, 14370–14380.
31. Erman, J. E., Vitello, L. B., Miller, A., and Kraut, J. (1992) Active-site mutations in cytochrome c peroxidase: A critical role for histidine-52 in the rate of formation of compound I. *J. Am. Chem. Soc. 114*, 6592–6593.
32. Erman, J. E., Vitello, L. B., Miller, M. A., Shaw, A., Brown, K. A., and Kraut, J. (1993) Histidine 52 is a critical residue for rapid formation of cytochrome *c* peroxidase compound I. *Biochemistry 32*, 9798–9806.
33. Goodin, D. B., Davidson, M. G., Roe, J. A., Mauk, A. G., and Smith, M. (1991) Amino acid substitutions at tryptophan-51 of cytochrome c peroixdase: Effects on coordination, species preference for cytochrome c, and electron transfer. *Biochemistry 30*, 4953–4962.
34. Neri, F., Indiani, C., Baldi, B., Vind, J., Welinder, K. G., and Smulevich, G. (1999) Role of the distal phenylalanine 54 on the structure, stability, and ligand binding of *Coprinus cinereus* peroxidase. *Biochemistry 38*, 7819–7827.
35. Roe, J., and Goodin, D. B. (1993) Enhanced oxidation of aniline derivatives by two mutants of cytochrome c peroxidase at tryptophan 51. *J. Biol. Chem. 268*, 20037–20045.
36. Gengenbach, A., Syn, S., Wang, X., and Lu, Y. (1999) Redesign of cytochrome c peroxidase into a manganese peroxidase: Role of tryptophans in peroxidase activity. *Biochemistry 38*, 11425–11432.
37. Badyal, S. K., Eaton, G., Mistry, S., Pipirou, Z., Basran, J., Metcalfe, C. L., Gumiero, A., Handa, S., Moody, P. C. E., and Raven, E. L. (2009) Evidence for heme oxygenase activity in a heme peroxidase. *Biochemistry 48*, 4738–4746.
38. Vitello, L. B., Erman, J. E., Miller, M. A., Mauro, M., and Kraut, J. (1992) Effect of Asp235→Asn substitution on the absorption spectrum and hydrogen peroxide reactivity of cytochrome c peroxidase. *Biochemistry 31*, 11524–11535.